

UNIVERSIDADE ESTADUAL DE CAMPINAS
SISTEMA DE BIBLIOTECAS DA UNICAMP
REPOSITÓRIO DA PRODUÇÃO CIENTÍFICA E INTELLECTUAL DA UNICAMP

Versão do arquivo anexado / Version of attached file:

Versão do Editor / Published Version

Mais informações no site da editora / Further information on publisher's website:

<https://www.sciencedirect.com/science/article/pii/S0308814619311550>

DOI: 10.1016/j.foodchem.2019.125053

Direitos autorais / Publisher's copyright statement:

©2019 by Elsevier. All rights reserved.

DIRETORIA DE TRATAMENTO DA INFORMAÇÃO

Cidade Universitária Zeferino Vaz Barão Geraldo

CEP 13083-970 – Campinas SP

Fone: (19) 3521-6493

<http://www.repositorio.unicamp.br>



Nanostructured lipid carriers loaded with free phytosterols for food applications

Valeria da Silva Santos^{a,*}, Bruno Brito Braz^a, Alan Ávila Silva^b, Lisandro Pavie Cardoso^c, Ana Paula Badan Ribeiro^b, Maria Helena Andrade Santana^a

^a Department of Biotechnological Processes, School of Chemical Engineering, University of Campinas, 500 Albert Einstein Ave., Campinas, SP 13083-970, Brazil

^b Department of Food Technology, School of Food Engineering, University of Campinas, 80 Monteiro Lobato St., Campinas, SP 13083-970, Brazil

^c Department of Applied Physics, Institute of Physics Gleb Wataghin, University of Campinas, 777 Sérgio Buarque de Holanda St., 13083-859 Campinas, SP, Brazil

ARTICLE INFO

Keywords:

Lipid nanoparticles
Free phytosterols
High oleic sunflower oil
Fully hydrogenated canola oil
Fully hydrogenated crambe oil
Thermal and crystalline behavior

ABSTRACT

The objective of this study was to develop nanostructured lipid carriers (NLCs) with free phytosterols (FP) using conventional fats and oils. Lipid matrices (LMs) and NLCs were produced with high oleic sunflower oil, fully hydrogenated canola (CA) and crambe (CR) oils by high-pressure homogenization (HPH). The NLCs were evaluated for hydrodynamic diameter (Z-ave), polydispersity index (PDI), and zeta potential (ZP). The melting behavior and polymorphism were investigated for both, the LMs and NLCs. The NLCs presented particle sizes ranging from 148.23 to 342.10 nm, PDI from 0.275 to 0.481, and ZP between -22.27 and -29.70 mV. The NLCs presented higher thermal resistance than that of the LMs. The use of CA and CR separately in the NLC formulations favored the incorporation of FP. The LMs and NLCs presented crystals in β -form and in mixtures of β' and β forms. The developed NLCs can be used for food enrichment, such as spreads, margarine, and beverages.

1. Introduction

The application of nanotechnology in the food area is quite recent, and it could be considered non-existent in terms of industrial application. Even the great potential for use has not been recognized. To date, the number of scientific studies focused on the development of nanosystems and their applications in food is still low; however, this number has been increasing with great potential for commercially viable applications in the near future (Beloqui, Solinis, Rodriguez-Gascon, Almeida, & Preat, 2016; Cerqueira et al., 2014; Lacatusu, Badea, Stan, & Meghea, 2012; Rashidi & Khosravi-Darani, 2011).

Most of the developments in nanotechnology in the food area occurred after 2005, when researchers started reporting several findings on nanoscale systems with the potential for food application. The highlighted topic in this field was the use of nanotechnology for the development of bioactive compound carriers for foods (Aditya et al., 2015; Santos, Ribeiro, & Santana, 2019; Weiss, Takhistov, & McClements, 2006). These discoveries were initially encouraged by the use of carrier systems in pharmaceutical and cosmetic fields, where nanotechnology had been widely explored and applied for the delivery of many drugs and bioactive compounds. Although the development of these nanosystems in the biomedical sectors has been successful, many

challenges such as the choice of raw materials must be overcome for food applications to be achieved since foods require compounds generally recognized as safe (GRAS) and/or under law limitations.

In this context, lipid nanosystems present great potential for food applications since a variety of natural and modified fats and oils are readily available for the food industry. In the scientific literature, it is possible to find a range of studies suggesting the development of solid lipid nanoparticles (SLNs) and nanostructured lipid carriers (NLCs) for the transport and protection of bioactive compounds, for food applications (Aditya et al., 2015). The main interest in transporting bioactive compounds in food lies in the development of enriched or functional food products, to provide healthy food for consumers.

Bioactive compounds are commonly known for their functional properties related to disease prevention. However, many of these compounds are naturally present in foods in very low amounts or with limited bioavailability. Currently, some of these compounds have been extracted from plant and animal sources to be directly incorporated in food. However, this direct incorporation generally provides low chemical stability and bioavailability, which may reduce the functional effects of these compounds. In addition, bioactive compounds often have low solubility, which makes their applications in food challenging (Vaikousi, Lazaridou, Biliaderis, & Zawistowski, 2007).

* Corresponding author.

E-mail addresses: santosilvaleria@hotmail.com (V.d.S. Santos), b.brito@campinas.br (B.B. Braz), alan_avila_dasilva@hotmail.com (A.Á. Silva), cardoso@ifi.unicamp.br (L.P. Cardoso), badanribeiro@gmail.com (A.P.B. Ribeiro), mariahelena.santana@gmail.com (M.H.A. Santana).

<https://doi.org/10.1016/j.foodchem.2019.125053>

Received 20 February 2019; Received in revised form 28 May 2019; Accepted 21 June 2019

Available online 21 June 2019

0308-8146/ © 2019 Elsevier Ltd. All rights reserved.

Lipid nanoparticles show promise for delivering lipid-soluble bioactive compounds with low water solubilities, such as carotenoids, tocopherols, omega-3 (ω -3), phytosterols, and are widely used as ingredients in various food products. In addition, lipid nanoparticles can be used to protect bioactive compounds from chemical degradation during food processing and storage. For instance, Awad, Helgason, Weiss, Decker, and McClements (2009) evaluated the thermal and polymorphic behaviors of SLNs developed with tripalmitin loaded fish oil, rich in ω -3. The results showed that fish oil, can be successfully incorporated into SLNs suspensions. The authors suggested that SLNs could be used to stabilize fish oils against oxidation by retarding molecular diffusion and keeping polyunsaturated lipids (ω -3) isolated from pro-oxidants. Lacatusu et al. (2013) studied NLCs developed with fish oil and tristearin for lutein transport. The authors concluded that the lutein into NLCs could serve to successfully incorporate this nutraceutical into water-dispersible food systems. Lacatusu et al. (2012) developed NLCs with combinations of grape seed oil, fish oil and squalene to transport β -sitosterol. All loaded-bio-active NLCs presented in this study has shown excellent physical stability. Another advantage observed in this study is associated with the main feature of the developed NLCs to manifest a better sitosterol-sustained release behavior as compared to their related nanoemulsions. Additionally, authors reported that lipid nanoparticles may improve the bioavailability and absorption of bioactive compounds in the gastrointestinal tract due to their relatively high contact surface area (Weiss et al., 2008).

As already cited, to date, studies have been carried out using purified lipid as raw materials, such as isolated fatty acids and triacylglycerols (TAGs) as well as bioactive compounds of analytical grade (e.g. β -sitosterol). These compounds make it difficult, particularly in terms of cost, to apply these systems in food products at an industrial scale.

Today, hardfats are being used as solid material for the development of SLNs and NLCs (Santos, Ribeiro, & Santana, 2017). Hardfats are fully hydrogenated vegetable oils, with melting points ranging from 40 to 72 °C. They are obtained when all the double bonds of fatty acids are saturated during the full catalytic hydrogenation of unsaturated oils. They were initially developed as raw materials to interesterify low-trans fats; recently, hardfats have also been used as structuring agents of liquid oils (Ribeiro, Basso, & Kieckbusch, 2013; Tamjidi, Shahedi, Varshosaz, & Nasirpour, 2013).

Notably, our research group pioneered the use of hardfats for the development of both SLNs and NLCs for the transport of food grade lipophilic bioactive compounds, such as phytosterols (FP) (Santos et al., 2017). Due to the health benefits of FP, our focus lies in transporting them as particles in food.

FP, also known as plant sterols, are the main sterol fraction in plant extracts and vegetable oils. More than 10 types of FP molecules can be naturally found, with β -sitosterol, Δ 5-avenasterol, campesterol, and stigmasterol being the main species. The proportion of each sterol in the total content varies according to the plant source (Gomes Silva et al., 2019). Regarding the bioactivity and consumption of FP by humans, studies have been carried out to demonstrate the positive effects of FP on metabolism (Kritchevsky & Chen, 2005). The first reported effect was the prevention of coronary disease. FP are known to compete with cholesterol for absorption due to their similarities, thereby leading to lower blood cholesterol levels (Ling and Jones, 1995; Ntanos, MacDougall, & Jones, 1998). Studies indicate that the consumption of 2 g of FP per day significantly reduces the cholesterol levels, and consequently prevents coronary heart diseases (Moruisi, Oosthuizen, & Opperman, 2013; Wu, Fu, Yang, Zhang, & Han, 2009). In addition, ingestion of FP has been associated with cancer prevention. Recent studies indicate that the prevention of cancer by the consumption of FP is related to the modulation of sterol biosynthesis, improvement of the immune response, and induction of tumor metastases (Shahzad et al., 2017).

From the technological point of view, our research group recently observed that food grade FP (composed of a mixture of phytosterols)

have thermal and crystalline behaviors that are quite similar to those of isolated FP, such as β -sitosterol and stigmasterol (Gomes Silva et al., 2019). In addition, previously, we developed NLCs composed of soybean oil and fully hydrogenated soybean oil with the incorporation of 30% FP, and these systems showed promise for food applications (Santos et al., 2017).

Thus, the central objective of this work was the development of NLCs with other conventional raw materials, such as high oleic sunflower oil (HOSO), and fully hydrogenated canola (CA) and crambe (CR) oils for food-grade FP transport.

2. Materials and methods

2.1. Materials

The solid lipid raw materials used for the development of lipid matrices (LMs) and NLCs were the fully hydrogenated canola (CA) and crambe (CR) oils provided by SGS Agricultura e Indústria Ltda© (Ponta Grossa – PR, Brazil). High oleic sunflower oil (HOSO), supplied by Cargill Agrícola S.A (Mairinque – SP, Brazil), was used as the liquid lipid in the NLCs composition.

HOSO presented 90.68% of unsaturated fatty acids, which consisted of 78.60% oleic acid (O, C18:1) and 11.41% linoleic acid (L, C18:2). The CA and CR oils presented 100% of saturated fatty acids. The predominant for CA composition was 93.82% of stearic acid (S, C18:0) and 5.24% of palmitic acid (P, C16:0), and for CR, 56.30% of behenic acid (Be, C22:0) and 31.70% of stearic acid (S, C18:0). The main TAGs present in the HOSO were: OOO representing approximately 65% of the total, followed by OLO (~15%) and OOP (~10%). CA presented 4 distinct TAGs, with the majority being SSS (~80%) and PSS (~13%). In CR, 9 different TAGs were found, among which the predominant ones were SBeBe (~38%), SSBe (~17%), and SABe (~17%). Ethoxylated sorbitan monooleate P1754 (Tween®80, T80), with a hydrophilic-lipophilic balance (HLB) of 14.0, was purchased from Sigma-Aldrich (St. Louis, Missouri, USA). The bioactive compounds were free FP, which were kindly provided by a national production initiative (still under development, located in Itajaí, Santa Catarina, Brazil). The FP obtained from soybean oil, were 98% pure, composed of a mixture of sterols, with β -sitosterol (~44%), stigmasterol (~27%), and campesterol (~23%) being the main sterols. The complete information can be found in the [Supplementary Material \(Table S.1 and S.2\)](#).

2.2. Methods

2.2.1. Formulation of lipid matrices and nanoparticles

The NLCs were developed with 10% (m/m) of the total lipid phase and 90% (m/m) of the aqueous phase. The aqueous phase was composed of distilled water and 2% of the T80 as the emulsifier, according to Santos et al. (2017) (Fig. 1C and D).

For the composition of the lipid phase, 14 lipid matrices were formulated with liquid lipid (HOSO in proportions of 20, 40, 50, and 70%), solid lipids (30 and 50% of CA and CR and their mixtures), and the bioactive compound (30 and 50% FP). Each LM was used for the development of the NLCs (Fig. 1).

2.2.2. Production of lipid matrices and nanoparticles

LMs were melted at 130 °C and the FP were gradually added, under magnetic stirring until complete melting of the FP was attained, not exceeding 3 min to avoid degradation of the bioactive compound. Subsequently, the solution was conditioned at 5 °C for 24 h, for lipid crystallization, followed by further conditioning for another 24 h at 25 °C for crystalline stabilization and subsequent physical evaluations.

The NLCs preparation was performed according to 4 steps: (i) fusion of the lipid fraction, (ii) formation of the emulsion, (iii) nanoemulsification, and (iv) crystallization of the lipid phase. The lipid fraction (10%) was melted and homogenized as previously described.

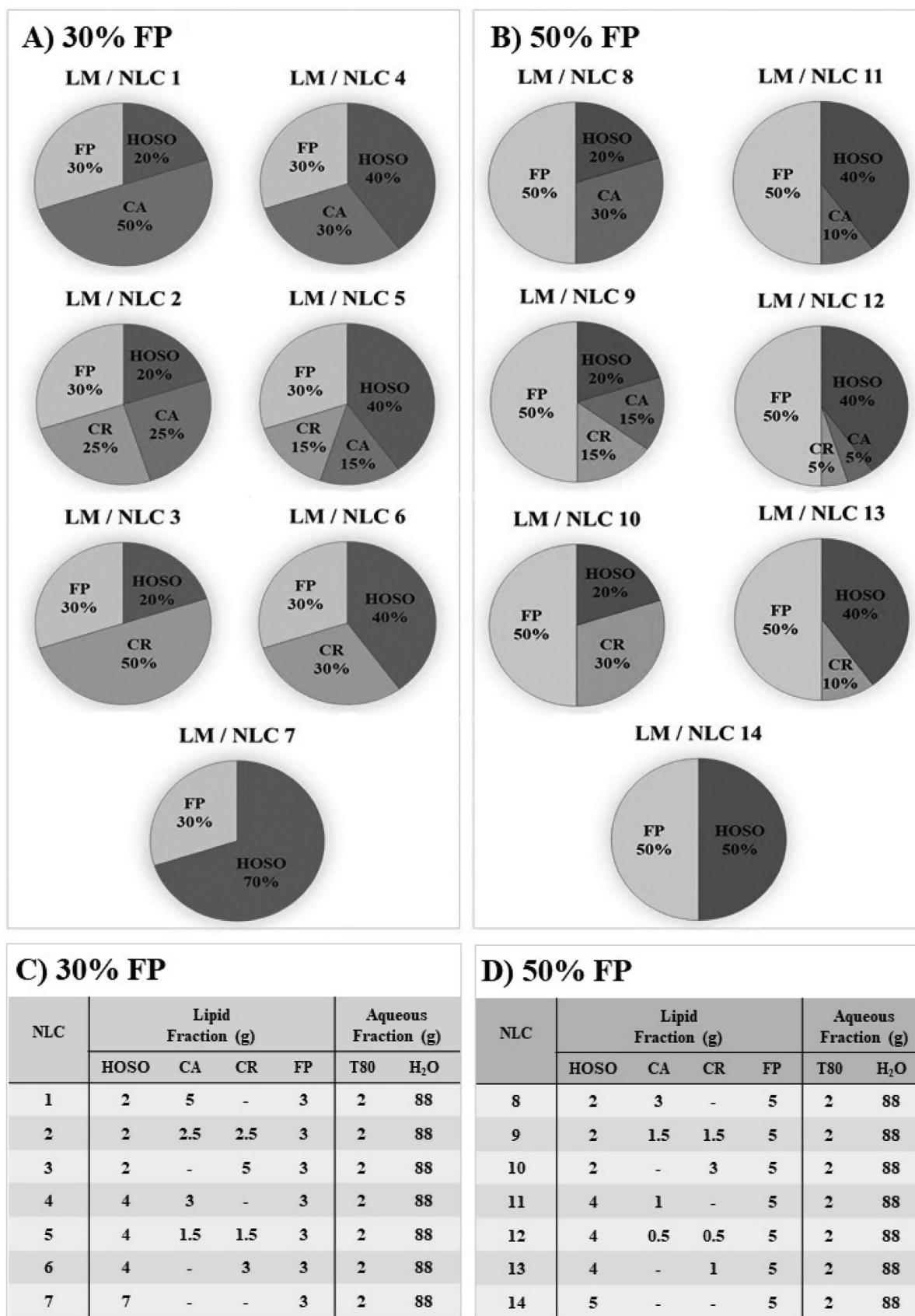


Fig. 1. Schematic representation of lipid matrices (LMs) composition, used in the nanostructured lipid carriers (NLCs) with free phytosterols (FP). A) LMs and NLCs, both developed with 30% FP, 20, 40 and 70% high oleic sunflower oil (HOSO), 15, 25, 30 and 50% of fully hydrogenated canola oil (CA) and crambe oil (CR); B) LMs and NLCs, both developed with 50% FP 20, 40 and 50% HOSO, 5, 10, 15 and 30% of CA and CR. C) Table containing the formulation of each nanoparticle with incorporation of 30% of FP, with the components divided into lipid and aqueous fractions, expressed in g/100 g. D) Table containing the formulation of each nanoparticle with incorporation of 50% of FP, with the components divided into lipid and aqueous fractions, expressed in g/100 g.

Table 1

Mean hydrodynamic diameter (Z-ave), polydispersity index (PDI) and zeta potential (ZP) of the nanostructured lipid carriers (NLC) with 30 and 50% of free phytosterols (FP) evaluated after 24 h, 15 days, 30 days and 60 days of production.

| NLC/Time | Z-ave (d.nm) | PDI | ZP (mV) | NLC/Time | Z-ave (d.nm) | PDI | ZP (mV) |
|----------|--------------------------------|-------------------------------------|-----------------------------------|----------|-------------------------------------|------------------------------|-----------------------------------|
| 24 h | 30% FP | | | 24 h | 50% FP | | |
| NLC 1 | 204.97 ± 3.45 ^{cdefB} | 0.410 ± 0.026 ^{abcA} | −28.30 ± 0.95 ^{hijklmB} | NLC 8 | 342.10 ± 30.00 ^{abcA} | 0.406 ± 0.055 ^{bA} | −23.57 ± 0.72 ^{bcdcfA} |
| NLC 2 | 250.00 ± 7.30 ^{aA} | 0.358 ± 0.027 ^{abA} | −24.40 ± 0.56 ^{cdeB} | NLC 9 | 217.10 ± 10.70 ^{hiB} | 0.481 ± 0.086 ^{abA} | −22.27 ± 0.92 ^{abA} |
| NLC 3 | 214.40 ± 6.91 ^{bcdB} | 0.310 ± 0.062 ^{ghijA} | −27.70 ± 0.98 ^{ghijklmB} | NLC 10 | 254.53 ± 05.49 ^{efghIA} | 0.362 ± 0.071 ^{bA} | −23.07 ± 0.93 ^{abcdA} |
| NLC 4 | 179.77 ± 3.74 ^{ijkB} | 0.321 ± 0.025 ^{efghjA} | −29.17 ± 0.21 ^{klmnB} | NLC 11 | 282.95 ± 23.35 ^{bcdcfghIA} | 0.378 ± 0.052 ^{bA} | −25.57 ± 0.32 ^{ghA} |
| NLC 5 | 184.70 ± 3.01 ^{ijkB} | 0.315 ± 0.031 ^{fgijB} | −28.37 ± 0.49 ^{ijklmB} | NLC 12 | 265.55 ± 18.15 ^{defghIA} | 0.384 ± 0.006 ^{bA} | −26.37 ± 0.85 ^{hijA} |
| NLC 6 | 177.33 ± 4.29 ^{kB} | 0.275 ± 0.028 ^{ijB} | −29.70 ± 1.35 ^{lmnB} | NLC 13 | 205.97 ± 03.79 ^{iA} | 0.392 ± 0.028 ^{bA} | −26.47 ± 0.42 ^{hijA} |
| NLC 7 | 148.23 ± 0.55 ^{mB} | 0.276 ± 0.025 ^{ijA} | −26.13 ± 0.46 ^{efgB} | NLC 14 | 246.00 ± 26.30 ^{efghIA} | 0.343 ± 0.059 ^{bA} | −24.73 ± 0.55 ^{cdefghA} |
| 15 days | | | | 15 days | | | |
| NLC 1 | 202.27 ± 4.42 ^{defgB} | 0.411 ± 0.004 ^{abA} | −27.83 ± 0.15 ^{ghijklmB} | NLC 8 | 482.75 ± 18.88 ^{aA} | 0.478 ± 0.055 ^{abA} | −26.60 ± 0.62 ^{hijA} |
| NLC 2 | 219.23 ± 2.46 ^{bB} | 0.384 ± 0.031 ^{abdefghA} | −29.27 ± 0.49 ^{klmnA} | NLC 9 | 385.29 ± 34.29 ^{abcdA} | 0.359 ± 0.039 ^{bA} | −29.60 ± 0.57 ^{klmA} |
| NLC 3 | 212.87 ± 2.10 ^{bcdB} | 0.399 ± 0.011 ^{abdeA} | −27.27 ± 0.71 ^{ghijkA} | NLC 10 | 281.60 ± 10.18 ^{bcdcfghIA} | 0.473 ± 0.126 ^{abA} | −28.00 ± 0.36 ^{ijkA} |
| NLC 4 | 184.77 ± 1.25 ^{ijkB} | 0.348 ± 0.200 ^{abdefghijB} | −28.00 ± 0.44 ^{ghijklmA} | NLC 11 | 382.50 ± 18.95 ^{bcdcfA} | 0.404 ± 0.007 ^{bA} | −31.55 ± 0.92 ^{nB} |
| NLC 5 | 190.10 ± 3.90 ^{hijB} | 0.360 ± 0.007 ^{abdefghA} | −27.10 ± 0.75 ^{ghijA} | NLC 12 | 368.20 ± 00.99 ^{bcdcfA} | 0.438 ± 0.089 ^{abA} | −29.37 ± 0.95 ^{klmB} |
| NLC 6 | 182.27 ± 1.21 ^{ijkB} | 0.305 ± 0.016 ^{ghijB} | −26.17 ± 0.47 ^{efghA} | NLC 13 | 230.20 ± 03.47 ^{ghIA} | 0.439 ± 0.030 ^{abA} | −28.97 ± 0.49 ^{klB} |
| NLC 7 | 152.77 ± 2.66 ^{lmB} | 0.268 ± 0.010 ^{jB} | −30.60 ± 0.35 ^{noA} | NLC 14 | 308.13 ± 42.93 ^{bcdcfghA} | 0.397 ± 0.075 ^{bA} | −31.13 ± 1.31 ^{lmnA} |
| 30 days | | | | 30 days | | | |
| NLC 1 | 201.83 ± 1.86 ^{efghB} | 0.411 ± 0.006 ^{abA} | −24.53 ± 0.49 ^{defA} | NLC 8 | 366.50 ± 25.70 ^{abcA} | 0.390 ± 0.028 ^{bA} | −23.83 ± 0.59 ^{bcdcfghB} |
| NLC 2 | 208.03 ± 3.40 ^{cdeB} | 0.347 ± 0.029 ^{abdefghijA} | −22.37 ± 0.71 ^{abA} | NLC 9 | 326.05 ± 23.12 ^{bcdcfghA} | 0.387 ± 0.025 ^{bA} | −24.80 ± 0.57 ^{cdefghB} |
| NLC 3 | 212.77 ± 1.23 ^{bcdB} | 0.390 ± 0.010 ^{abdefB} | −21.50 ± 0.20 ^{abB} | NLC 10 | 328.87 ± 02.75 ^{bcdcfghA} | 0.444 ± 0.005 ^{abA} | −25.73 ± 0.59 ^{ghA} |
| NLC 4 | 191.40 ± 8.39 ^{ghijB} | 0.301 ± 0.032 ^{hijB} | −29.90 ± 1.35 ^{mnB} | NLC 11 | 245.60 ± 21.92 ^{efghIA} | 0.466 ± 0.031 ^{abA} | −22.65 ± 0.35 ^{abcA} |
| NLC 5 | 190.47 ± 4.80 ^{ghijB} | 0.338 ± 0.008 ^{bcdcfghijB} | −20.30 ± 1.04 ^{abA} | NLC 12 | 251.00 ± 00.89 ^{efghIA} | 0.612 ± 0.096 ^{abA} | −24.47 ± 0.74 ^{cdefghB} |
| NLC 6 | 187.43 ± 2.53 ^{ijkB} | 0.345 ± 0.020 ^{abdefghijB} | −27.27 ± 0.67 ^{ghijkA} | NLC 13 | 236.57 ± 02.80 ^{ghIA} | 0.448 ± 0.300 ^{abA} | −29.97 ± 0.35 ^{klmnB} |
| NLC 7 | 161.47 ± 1.00 ^{jB} | 0.330 ± 0.014 ^{defghijA} | −35.60 ± 0.10 ^{pB} | NLC 14 | 286.67 ± 27.45 ^{bcdcfghIA} | 0.354 ± 0.041 ^{bA} | −28.33 ± 0.46 ^{klA} |
| 60 days | | | | | | | |
| NLC 1 | 208.93 ± 4.23 ^{bcdB} | 0.423 ± 0.006 ^{aA} | −21.87 ± 0.35 ^{abA} | NLC 8 | 337.75 ± 05.35 ^{bcdA} | 0.419 ± 0.057 ^{bA} | −24.70 ± 0.70 ^{cdefghB} |
| NLC 2 | 206.93 ± 4.8 ^{cdeB} | 0.375 ± 0.048 ^{abdefghA} | −21.43 ± 0.55 ^{abA} | NLC 9 | 375.65 ± 25.10 ^{abA} | 0.456 ± 0.095 ^{abA} | −25.27 ± 0.29 ^{efghB} |
| NLC 3 | 214.87 ± 2.32 ^{bcB} | 0.408 ± 0.016 ^{abcdA} | −32.50 ± 0.70 ^{oB} | NLC 10 | 294.85 ± 29.75 ^{bcdcfghIA} | 0.460 ± 0.052 ^{abA} | −21.07 ± 0.75 ^{aA} |
| NLC 4 | 186.77 ± 3.36 ^{ijkB} | 0.331 ± 0.023 ^{cdefghijB} | −26.67 ± 0.40 ^{fgiB} | NLC 11 | 273.27 ± 32.00 ^{cdefghIA} | 0.429 ± 0.055 ^{abA} | −25.10 ± 0.52 ^{defghA} |
| NLC 5 | 193.17 ± 3.61 ^{ghijB} | 0.345 ± 0.032 ^{abdefghijA} | −24.93 ± 0.40 ^{defB} | NLC 12 | 258.67 ± 20.90 ^{efghIA} | 0.382 ± 0.045 ^{bA} | −23.27 ± 0.64 ^{bcdA} |
| NLC 6 | 188.03 ± 1.14 ^{ijkB} | 0.368 ± 0.005 ^{abdefghB} | −23.27 ± 0.67 ^{bcdA} | NLC 13 | 239.07 ± 04.27 ^{ghIA} | 0.485 ± 0.050 ^{abA} | −31.37 ± 0.71 ^{mnB} |
| NLC 7 | 160.60 ± 0.95 ^{jB} | 0.341 ± 0.020 ^{bcdcfghijA} | −26.37 ± 0.61 ^{efghIA} | NLC 14 | 270.10 ± 32.57 ^{cdefghIA} | 0.355 ± 0.021 ^{bA} | −25.83 ± 1.10 ^{ghIA} |

*Average of three replicates ± Standard Deviation; Different lowercase letters in the same column indicate significant difference related to the evaluation of each parameter (Z-ave, PDI and ZP) in comparison to the time of production of NLC (24 h, 15, 30 and 60 days after processing), at the probability level ($p \leq 0.05$) according to the Tukey Test; Capital letters on the same line indicate a significant difference in probability ($p \leq 0.05$) according to the Tukey Test related to the comparison between the NLC produced with different levels of incorporation of the bioactive compound (30 and 50% of FP) for each parameter (Z-ave, PDI and ZP).

Subsequently, the aqueous phase (90%) was added at 90 °C and the pre-emulsion was obtained in Ultra Turrax IKA T18 Basic (Germany) at 20,000 rpm for 3 min. Afterward, the pre-emulsion was subjected to 3 cycles of homogenization at 800 bar in a high-pressure homogenizer (HPH, GEA Niro Soavi, model: NS 1001L PANDA 2K, Italy), as recommended by Santos et al. (2017).

After the HPH process, the obtained nanoemulsions were stored for 24 h at 5 °C for lipid fraction crystallization and for obtaining the dispersions containing the NLCs, which were subsequently stored at 25 °C for 24 h, for crystalline stabilization. A portion of the samples in aqueous suspension was maintained at 25 °C for the initial characterization and stability evaluation over 60 days of storage and another portion was dried by lyophilization, as described in the following sequence.

2.2.3. Additional drying process of nanoparticles

The NLCs in aqueous suspension, shortly after the crystallization and stabilization process described in the previous item, were frozen in an ultra-freezer (−86 °C) for 2 h, after which they were immediately subjected to lyophilization for 24 h at −25 °C, under a vacuum of 0.370 mbar using a lyophilizer (Liobras L101, Brazil). The NLCs were stored at 25 °C for further characterization.

2.2.4. Characterization of lipid matrices and nanoparticles

2.2.4.1. Size, polydispersity index, and zeta potential of nanoparticles. The NLCs in the aqueous dispersions were evaluated in triplicate for particle size using the hydrodynamic diameter (Z-ave) in nanometers (d nm),

polydispersity index (PDI), and zeta potential (ZP) after 24 h, 15, 30, and 60 days of the production process by dynamic light scattering (DLS, Zetasizer Nano NS, Malvern, UK). The samples were diluted with distilled water to reduce the opalescence before the measurements. Data analysis was performed using the software included in the equipment system.

2.2.4.2. Thermal behavior in the melting of lipid matrices and nanoparticles. The melting thermal behavior of the LM and the bioactive compounds used to produce NLCs, as well as lyophilized NLCs, were analyzed using the TA Instruments, model Q2000, attached to the RCS90 Refrigerated Cooling System (TA Instruments, Waters LLC, New Castle). The data were processed in the Universal V4.7A software (TA Instruments, Waters LLC, New Castle). The LMs used for the production of NLCs were packed in aluminum hermetic capsules (~10 mg) and melted at 150 °C to erase the crystalline history. Afterwards, they were subjected to the same thermal treatment performed on the NLCs after subjection to HPH (the crystallization and stabilization stages (at 5 °C and for 24 h; at 25 °C and for 24 h)), thus making it possible to compare the results during melting. The melting events were evaluated under isothermal conditions (at 25 °C and for 10 min), followed by heating to 25 °C at a rate of 10 °C/min (Wang et al., 2014).

To evaluate the melting thermal behavior of the NLCs, the lyophilized samples (mass of ~10 mg) were packed in hermetic aluminum capsules and submitted to the same DSC program mentioned earlier.

For all melting analysis, the following parameters were obtained: initial melting temperature (T_{in}), peak melting temperature (T_{max}), final melting temperature (T_{off}), and melting enthalpy (ΔH_m).

2.2.4.3. X-ray diffraction analyses of lipid matrices and nanoparticles. X-ray diffraction (XRD) analysis was performed on the LMs used in nanoparticles production, on the lyophilized NLCs, and bioactive compound (FP) according to the AOCS method Cj 2-95 (AOCS, 2009).

The FP and LMs were subjected to thermal treatment under the same conditions of the crystallization and stabilization of NLCs after the production process in HPH. Thus, the LMs and the FP were melted at 150 °C and conditioned at 5 °C for 24 h, followed by 24 h at 25 °C.

The NLCs were subjected to XRD analysis after lyophilization. All XRD analyses were performed using a Philips diffractometer (PW 1710) using Bragg-Brentano (θ : 2θ) geometry with Cu- α rad radiation ($\lambda = 1.54056 \text{ \AA}$, 40 KV voltage, and 30 mA current).

The measurements were obtained with steps of 0.02° in 2° and an acquisition time of 2 s, with scans of 1.8–40° (2° scale), at 25 °C. The identification of the polymorphic forms of the LM and NLCs were performed according to the typical short spacings of the lipid crystals (AOCS, 2009), and the peaks of the FP were enumerated and compared with results found in the literature.

2.2.5. Statistical analysis

Z-ave, PDI, and ZP data were statistically analyzed by One-Way Analysis of Variance (ANOVA) with Statistica (V.12) Software (Statsoft Inc., Tulsa, UK). The Tukey test was applied to determine the significant differences between the means at a probability level of 5% ($p \leq 0.05$).

3. Results and discussion

3.1. Size, polydispersity index, and zeta potential of the nanoparticles

The results obtained for Z-ave, PDI, and ZP for the NLCs developed with 30 and 50% FP are described in Table 1 and shown graphically in Supplementary Material (Fig. S.1). These parameters used together can provide information about the system stability.

The PDI values vary between 0 (monodisperse) and 1 (polydisperse) (Awad et al., 2009). ZP values over |30| mV, characterize colloidal systems with good stability, with |60| mV being the optimum. The system is considered susceptible to destabilization and the occurrence of limited flocculation between 5 and 30 mV (Madureira et al., 2016).

The NLCs with 30% FP presented lower values of Z-ave compared to those of the NLCs developed with 50% FP, which are statistically different ($p \leq 0.05$). The Z-ave values of the particles obtained shortly after processing (24 h), for the NLCs with 30 and 50% FP, ranged from 148.23 to 250.00 nm and 205.97 to 342.10 nm, respectively. The values for PDI were also lower for the NLCs with 30% FP, ranging from 0.275 to 0.410, compared to 0.343 to 0.481 for the NLCs with 50% FP (Fig. 2C and D). For the ZP results, values closer to 30 mV were obtained for the NLCs obtained with 30% FP, ranging from −24.40 to −29.70 mV, whereas for the 50% FP incorporation, these values were −22.27 at −26.47 mV (Table 1).

Similar values were obtained in the NLCs composed of solid lipids (palmitic and stearic fatty acids) and liquid lipids (squalene, grape seed oil, and fish oil) by I. Lacatusu et al. (2012) with the incorporation of 1% β -sitosterol, using T80. These NLCs had Z-ave values varying between 177 and 236 nm; PDI, from 0.225 to 0.380; and ZP, between −38 and −52 mV. Notably, the NLCs developed by these authors contained only 1% of β -sitosterol. In the present work, one of the challenges was the high incorporation of FP (30 and 50% of the lipid fraction) into the NLCs, representing 3 and 5% of FP in final systems, respectively.

In general, from the particle size distributions in Supplementary Material (Figs. S.2 and S.3), expressed in terms of scattered light intensity, “*I distribution*,” the proportional diameter to the sixth power

(Iad^6) is observed. It is possible to verify that the NLCs with 30% FP had greater stability over time when compared to the stability of those with 50% FP, even with a bimodal distribution. The differences between the two systems can be better understood by observing the graph related to the particle size distributions in terms of the number of particles, “*N distribution*,” proportional to the predominant diameter in the sample (Nad). Thus, it was possible to verify that the NLCs with 30% FP presented more homogeneous particle sizes, whereas for those with 50% of FP, a greater polydispersity between the particles was noticed. In addition, it should be noted that the polydispersity of the particles with 50% FP increased over time. It was observed that during the 60 days of evaluation, the Z-ave values of the NLCs with the 30% FP remained very similar. In addition, it was found that the increase in HOSO in the NLC with 30% FP favored the reduction of the particle size. All NLCs developed with 40% HOSO showed Z-ave values below 200 nm (NLC 4, 5 and 6). Notably the NLC with the lowest values of particle size was NLC 7, which was composed only of liquid lipid and the bioactive compound (70% of HOSO and 30% of FP) (Table 1).

The differences between the values showed that the TAG composition of LM directly interfere in the characteristics of the NLC system. In this way, we can verify that it is very important to explore LMs composed of different vegetable fats and oils, to extend the range of raw materials compatible with the use in NLC and SLN, as well as, to verify the best options for the incorporation of each bioactive compounds. It was found that NLC 2, composed of the mixture of CA and CR (25:25 m/m), HOSO (20%), and 30% FP showed particles with 250 nm after 24 h, and this value was reduced to 219.23 nm after 15 days, and after 30 days of storage further reduction to 212.77 nm was verified; all changes with statistical differences at a 5% probability level. Other reductions of Z-ave were detected in the NLCs with 30% FP, although they were not as intense as in NLC 2, and were not statistically different.

The NLCs with 50% FP showed many changes of Z-ave and PDI during 60 days of storage, and it was not possible to evaluate the influence of the increment in HOSO, as well as the chemical composition of the hardfats of the systems. It was observed that the incorporation of 50% FP negatively influenced the stability of the developed systems, except for NLC 13 that presented sizes between 200 and 300 nm without many variations over time. The ZP of this system increased from −26 to −31 mV approximately, indicating that this system, which was also developed with 50% FP, exhibits greater stability than the others do. The behavior of this system can be observed in Supplementary Material (in the results concerning the particle number distribution as a function of diameter (Nad)). It is possible to verify only one peak, indicating that the system is monodisperse, with less destabilization tendency.

The variations in the Z-ave values of the nanostructured particles, as observed for the NLCs developed with 30% FP and this phenomenon have been related to TAG polymorphic changes during storage. Bunjes and Unruh (2007) and Salminen, Helgason, Kristinnsson, Kristbergsson, and Weiss (2013) reported in their works that Z-ave reductions occurs due to the changes in the shape of lipid nanoparticles, and they correlated these reductions to the polymorphic transitions of the lipid content to a more stable form ($\alpha \rightarrow \beta' \rightarrow \beta$). Thus, after the emulsification process, the lipids were dispersed in water as droplets surrounded by the emulsifier. After the crystallization of the lipid fraction, solid and spherical nanoparticles, nanostructured by TAGs in the most unstable polymorphic form (α), were obtained. However, during storage, due to the polymorphic transitions of TAGs to the more stable form (β), the spherical nanoparticles become elongated in platelets forms. The ability of the lipids to crystallize in different forms will be better elucidated in the topic related to XRD.

3.2. Melting behavior of the free phytosterols, lipid matrix, and nanoparticles

The FP showed only one melting peak at T_{max} of 130.29 °C and

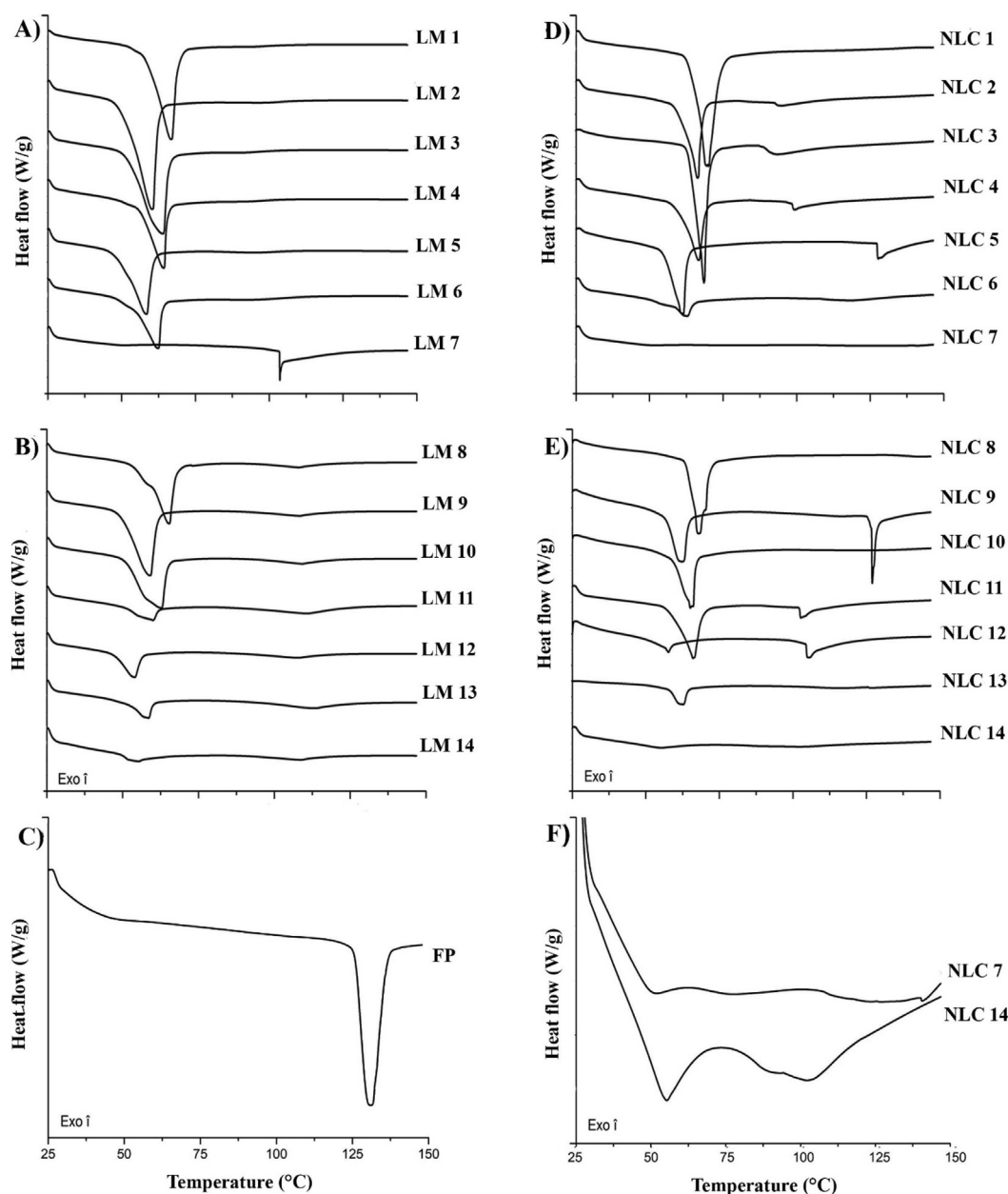


Fig. 2. Curves of the melting behavior of: A) Lipid matrices (LMs) containing 30% of free phytosterols (FP); B) Lipid matrices (LMs) containing 50% of FP; C) FP; D) NLCs containing 30% of FP; E) NLCs containing 50% of FP; F) Zoom of the melting curves of the NLC 7 and NLC 14.

melting range from 126.12 °C (T_{im}) to 136.14 °C (T_{off}), indicating that all FP components have similar melting properties (Fig. 2C). As described in the Materials section, the FP used in this study are food grade and have a mixture of FP in their composition. When comparing the thermal behavior of the components in the FP mixture with that of the components in the purified form, we can verify that the melting point of the pure components is higher, being 141.60 °C for β -sitosterol (Villaseñor, Angelada, Canlas, & Echegoyen, 2002), 169.20 °C for stigmasterol (Gomes Silva et al., 2019), and 140.50 °C for campesterol (Li, Ho, Li, Tao, & Tao, 2000).

The LMs developed with 30% FP presented only one melting peak, with T_{max} ranging from ~57 to ~67 °C, as shown in Fig. 2A. This behavior indicated the complete incorporation and solubilization of FP in these LMs. Thus, it can be affirmed that the crystallinity of FP was reduced, being more pronounced in the LM composed of the mixture of hardfats and HOSO. For LM 7, formulated only with liquid lipid (70% HOSO), the T_{max} was much higher than those in the other LMs

($T_{max} = 103.37$ °C) (Table S.3, Supplementary Material).

Two melting peaks were observed for all LMs containing 50% FP. The first was found in the region between 47 and 82 °C, probably indicative of the melting of the hardfat, HOSO, and FP mixtures, while the second peak was found between 87 and 127 °C, with lesser intensity than the first. This second peak can be related to the melting of the FP fraction that was not incorporated in LM, probably due to solubility (Fig. 2B).

In addition, changes in peak intensities were observed with increasing HOSO from 20 to 40% in both LMs with 30 and 50% FP incorporation. This effect can be observed through the ΔH_m of the LM systems containing 20% HOSO since they required relatively high energies for the phase transition. For the LMs with 30 and 50% FP, we obtained values of approximately -70 to -89 J/g and -45 to -50 J/g for incorporation of 20% HOSO and -43 to -53 and -9 to -14 J/g for 40% HOSO, respectively (Table S.3, Supplementary Material). This effect was even higher for the LMs developed with 70% (LM 7) and 50%

(LM 14) of HOSO with ΔH_m values of -16.67 and -7.22 J/g, respectively. It was verified that the HOSO contributed to the reduction in the crystallinity of these LMs, developed with high melting point components, such as FP. In addition, it should be noted that all the developed systems showed melting temperatures over the body temperature, allowing the use of all LMs for NLC applications. This temperature ($\pm 37^\circ\text{C}$) indication is based on their ability to maintain the particle structural integrity, according to recommendations found in the literature (Sharma, Diwan, Sardana, & Dhall, 2011; Tamjidi et al., 2013).

Additionally, as seen in the thermal behaviors of LM 7 and 14, lipophilic bioactive compounds, such as FP, which have high melting points, can be used as a solid lipid to compose the LM of NLC. These compounds present differentiated properties of fusion, such as the high thermal resistance (above 100°C), which allows their use for the development of NLC, for application in food, which will be thermally processed at high temperatures.

Comparing the melting behavior of the NLCs with those of the correspondent LMs, it was possible to verify that all the NLCs had higher T_{\max} than the LMs. This behavior was also observed by Tamjidi et al. (2013). Therefore, we can affirm that the developed NLCs presented higher thermal resistance than their respective LMs. Basically, the nanostructured systems required more energy to for phase transitions (solid-liquid) than the lipid systems did in macro-scale. It is suggested that in the NLCs, the TAGs constituents of the lipid fraction were organized in a more compact crystalline structure, thereby conferring greater thermal resistance to the nanoparticles. In contrast, in the macroscale, TAGs have relatively large spaces for their organization and formation of less compact crystalline networks.

In Fig. 2D, it is possible to visualize the melting thermal behavior of the NLCs developed with 30% FP. It was noted that NLC 1 and NLC 6 showed only one melting peak (T_{\max} of 70.08 and 62.65°C , respectively) (Table S.3, Supplementary Material), indicating that all components of these nanoparticles exhibited similar melting behaviors. However, in the other NLCs developed with 30% FP, a further melting peak was verified. It is suggested that in NLCs 2, 3, and 4, the second peak is related to the melting of the nanoparticles formed only by the FP covered by the emulsifier. Another suggestion related to the second peak would be the fusion of nanoparticles of smaller sizes present in the system, which require relatively high temperatures for the phase transition. However, in NLC 5, it is suggested that the undesired expulsion of the bioactive compound occurred since the T_{\max} of this peak (127.73°C) is very close to the FP T_{\max} (130.29°C). In NLC 7, developed only with FP and HOSO, 3 melting peaks with low ΔH_m values were verified, as can be seen in Fig. 2F. These peaks indicate that the formation of FP particles with different thermal melting behaviors occurred, which may be related to the Z-ave of the particles and not the expulsion of the FP since a pronounced peak was not observed in the region of 130°C .

Thus, these peaks may confirm the possible formation of nanoparticles composed only by FP, suggested in the first hypothesis, or the presence of FP in suspension, for NLC 5. However, these behaviors did not compromise the physical stability of the systems during 60 days of storage, as previously discussed. Notably, the best Z-ave, PDI, and ZP were obtained for the NLC with 30% FP (Table 1). Thus, the NLCs developed with CA, CR, and HOSO showed promise for the delivery of 30% FP in food.

Another point to highlight in this study was the eutectic effect observed in the LMs and NLCs developed with the mixture of CA and CR in both incorporation levels of 30% and 50% FP. The eutectic effect is directly related to incompatibilities between the constituents of the systems and may be associated with differences between the molecular volumes, preferred forms and/or polymorphs, resulting in a consequent reduction of the melting temperature compared to the isolated components (Himawan, Starov, & Stapley, 2006). Highlighting the eutectic effect, which may be beneficial for the development of SLNs and NLCs, with less compact crystalline nanostructures, which may favour the

incorporation of bioactive compounds. However, in the present study, the eutectic effect observed for the solid lipids mixture in the formulations did not contribute to the incorporation of FP into the NLCs. As can be observed in Fig. 2E, in the NLC 9 with 50% FP, were identified the presence of two melting peaks. The second peak being quite evident and is related to the expulsion of the bioactive compound, and the T_{\max} of 126.85°C , which is very close to the value obtained for the T_{\max} of the FP (130.29°C).

In the NLCs developed with 50% FP with the isolated use of the CA or CR (NLC 8, NLC 10, and NLC 13), only one melting peak was verified, proving that the use of these isolated hardfats is more effective for the development of NLCs with 30 and 50% FP. However, in general, the NLCs developed with 50% FP presented many changes of Z-ave, PDI, and ZP, as previously seen in the results obtained through DLS. Notably, the thermal behavior of NLC 13, composed of 10% CR and 40% HOSO, evidenced it as the best system to transport the 50% FP even after 60 days of the physical stability evaluation.

3.3. X-ray diffraction analyses of lipid matrices and nanoparticles

Lipids can crystallize in different crystalline structures, resulting in different molecular packagings. According to the current polymorphic nomenclature for TAGs, there are three specific types of sub-cells referring to polymorphs: α , β' , and β , denominated according to the classification of Brava Networks, as hexagonal, perpendicular orthorhombic, and triclinic crystals, respectively. In addition, lipids exhibit monotropic polymorphic transitions, which are processes of irreversible transitions from less stable polymorphic form to the more stable forms ($\alpha \rightarrow \beta' \rightarrow \beta$) (Martini, Awad, & Marangoni, 2006; Sato, 2001). These forms exhibit characteristic peaks, with the α -form having a single peak at 4.15 \AA ; the β' -form is characterized by two diffraction lines at 3.8 and 4.2 \AA ; and the β -form is related with a relatively high intensity line at 4.6 \AA and low intensity peaks at 3.7 and 3.8 \AA (Rousseau & Marangoni, 2002).

For the FP, a series of peaks were identified, with theta-2theta ($\theta:2\theta$) values of $5.20, 12.18, 12.80, 15.08, 15.80, 16.92, 17.86, 18.64, 19.70, 20.88, 21.82, 22.96, 24.06$, and 25.28 . In addition, in a recent study conducted by our research group, it was found that FP had a diffraction pattern that was very similar to those of pure sterols (Gomes Silva et al., 2019). Thus, it was verified that β -sitosterol, the main sterol in the FP mixture, crystallizes into a simple orthorhombic form, according to the crystallographic information verified through the Structural Database-CSD, with registration in CCDC 933712.

The crystalline structure of FP is very similar to the β' -form of TAG, which is classified as perpendicular orthorhombic, differing only in the angles of crystallization and in the deformations of the unit cells, where the simple orthorhombic form is deformed on one side of the square and the orthorhombic perpendicularly shows the deformation along the diagonal of the base square. Consequently, some FP peaks showed very similar diffraction patterns to those used for the identification of the polymorphs in the TAG. It is possible to observe in Fig. 3 a schematic representation of the 3 most common polymorphs of TAG (Fig. 3A) and the XRD peaks of FP with the identification of each peak and their respective 2θ values and d-spacing (Fig. 3B). Thus, it was possible to visualize the overlapping of the FP diffractograms with each α , β' , and β form characteristic of the TAGs. The peaks of FP that overlapped with the TAG peaks were peaks 9, 11, 12, and 13, with d-spacing of $4.62, 4.15, 3.97$, and 3.79 \AA , respectively (Fig. 3).

Therefore, possible identification of the crystalline forms of the TAGs with the respective overlapping peaks of the FP were performed, as described in Table 2.

It was observed that in the diffraction patterns of LMs and NLCs, the peaks related to FP had low intensities, as shown in Fig. 3. It is suggested that the intensity of the FP peaks was reduced by the incorporation, solubilization, and co-crystallization effects of the FP with the lipid materials. Moreover, no diffraction lines were observed at

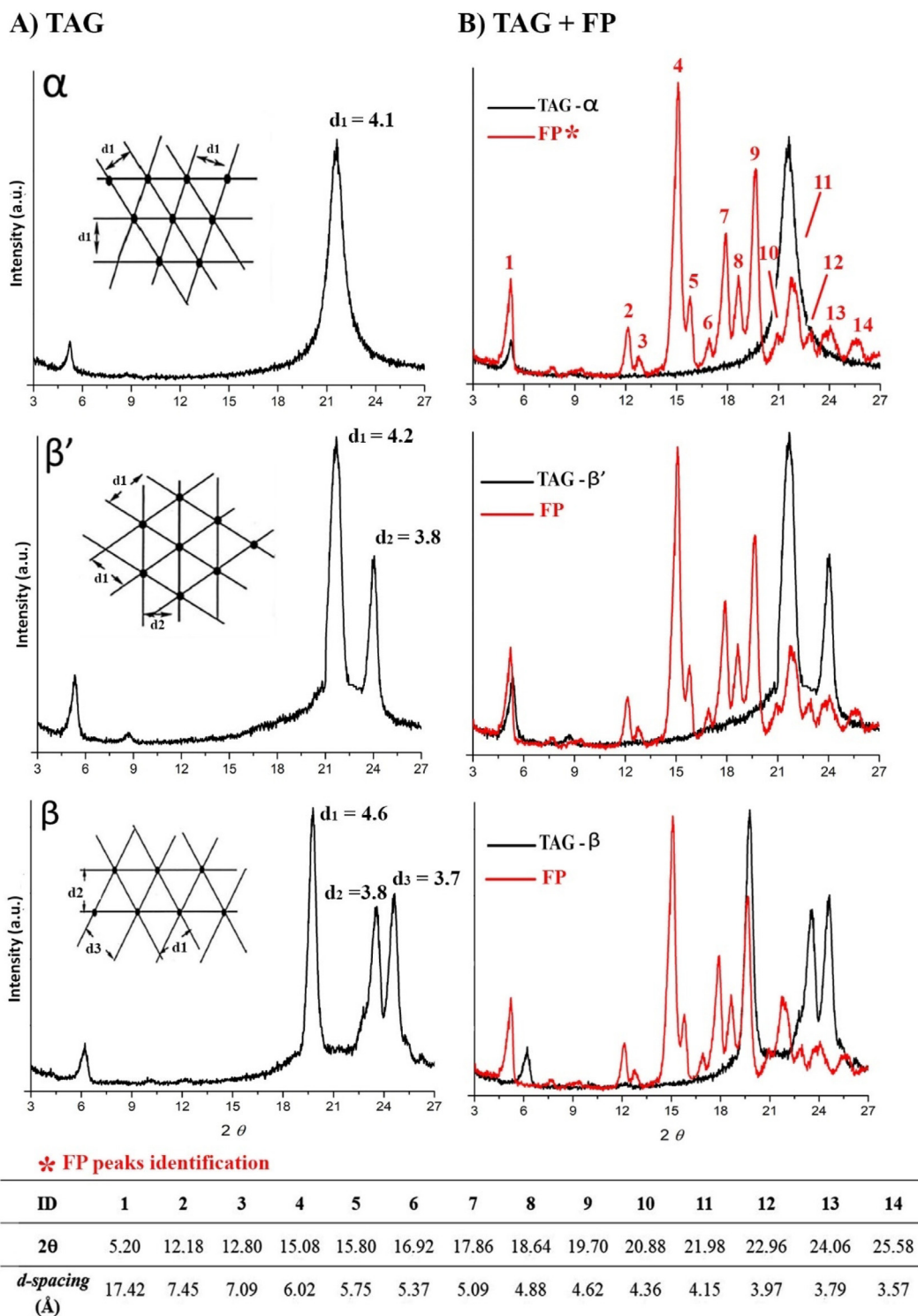


Fig. 3. Schematic representation of: (a) X-ray diffraction (XRD) patterns for triacylglycerols (TAG) in the most commonly polymorphic forms α , β' and β ; B) Experimental XRD patterns and peak identification of the free phytosterols (FP) with the peaks overlapping each TAG polymorphic form.

4.15 Å, which was indicative of the α -form of the TAG and the FP peak 11.

The results showed that both LMs and NLCs presented possible crystalline forms of the intermediate crystallization form (β'), in the most stable form (β) and the mixture of β' and β forms, as can be seen in Table 2. Furthermore, LMs developed only with HOSO and 30 and 50% FP, with LM 7 and LM 14, respectively, presented similar diffraction patterns. When comparing the distances from the baseline of the

respective NLCs, it is possible to observe a greater distance from the baseline, which may indicate a lower crystallinity when nanostructured (Fig. 4).

The LMs with the incorporation of FP in the proportions of 30 and 50% were found to have the same crystalline forms. Only LM 5 and LM 12, composed of the mixture of CA and CR, were different, where the presence of 50% FP favored the polymorphic transition from $\beta' + \beta$ to β (Table 2). Comparing the NLCs with 30% FP with the respective LMs,

Table 2

Short spacings and peak intensities of the diffractograms obtained for lipid matrices (LM) and nanostructured lipid carriers (NLC), developed with free phytosterols (FP), and polymorphic forms related to the triacylglycerol (TAG) crystalline behavior.

| Samples | Short spacings (Å) | | | | Polymorphic form of TAG |
|--|---|-----------|--------------------|--------------------|-------------------------|
| | 4.6 | 4.2 | 3.8 | 3.7 | |
| Lipid matrix – 30% FP | | | | | |
| LM 1 | 4.60(TAG ^{**})/4.62(FP ^{***}) | – | 3.89(TAG)/3.97(FP) | 3.73(TAG)/3.79(FP) | β |
| LM 2 | 4.63(TAG)/4.62(FP) | 4.22(TAG) | 3.81(TAG)/3.97(FP) | 3.73(TAG)/3.79(FP) | $\beta' + \beta$ |
| LM 3 | 4.68(TAG)/4.62(FP) | 4.21(TAG) | 3.81(TAG)/3.97(FP) | – | $\beta' + \beta$ |
| LM 4 | 4.60(TAG)/4.62(FP) | – | 3.86(TAG)/3.97(FP) | 3.71(TAG)/3.79(FP) | β |
| LM 5 | 4.61(TAG)/4.62(FP) | 4.20(TAG) | 3.89(TAG)/3.97(FP) | 3.70(TAG)/3.79(FP) | $\beta' + \beta$ |
| LM 6 | 4.64(TAG)/4.62(FP) | 4.20(TAG) | 3.80(TAG)/3.97(FP) | – | $\beta' + \beta$ |
| LM 7 ^{***} | – | – | – | – | – |
| Lipid matrix – 50% FP | | | | | |
| LM 8 | 4.61(TAG)/4.62(FP) | – | 3.87(TAG)/3.97(FP) | 3.73(TAG)/3.79(FP) | β |
| LM 9 | 4.66(TAG)/4.62(FP) | 4.20(TAG) | 3.84(TAG)/3.97(FP) | – | $\beta' + \beta$ |
| LM 10 | 4.66(TAG)/4.62(FP) | 4.20(TAG) | 3.81(TAG)/3.97(FP) | – | $\beta' + \beta$ |
| LM 11 | 4.61(TAG)/4.62(FP) | – | 3.88(TAG)/3.97(FP) | 3.71(TAG)/3.79(FP) | β |
| LM 12 | 4.60(TAG)/4.62(FP) | – | 3.87(TAG)/3.97(FP) | 3.70(TAG)/3.79(FP) | β |
| LM 13 | 4.65(TAG)/4.62(FP) | 4.20(TAG) | 3.80(TAG)/3.97(FP) | – | $\beta' + \beta$ |
| LM 14 ^{***} | – | – | – | – | – |
| Lyophilized nanostructured lipid carriers – 30% FP | | | | | |
| NLC 1 | 4.63(TAG)/4.62(FP) | – | 3.89(TAG)/3.97(FP) | 3.73(TAG)/3.79(FP) | β |
| NLC 2 | 4.64(TAG)/4.62(FP) | – | 3.89(TAG)/3.97(FP) | 3.73(TAG)/3.79(FP) | β |
| NLC 3 | – | 4.21(TAG) | 3.80(TAG)/3.97(FP) | – | β' |
| NLC 4 | 4.64(TAG)/4.62(FP) | – | 3.88(TAG)/3.97(FP) | 3.74(TAG)/3.79(FP) | β |
| NLC 5 | 4.63(TAG)/4.62(FP) | – | 3.86(TAG)/3.97(FP) | 3.72(TAG)/3.79(FP) | β |
| NLC 6 | – | 4.20(TAG) | 3.80(TAG)/3.97(FP) | – | β' |
| NLC 7 ^{***} | – | – | – | – | – |
| Lyophilized nanostructured lipid carriers – 50% FP | | | | | |
| NLC 8 | 4.66(TAG)/4.62(FP) | – | 3.89(TAG)/3.97(FP) | 3.73(TAG)/3.79(FP) | β |
| NLC 9 | 4.62(TAG)/4.62(FP) | – | 3.88(TAG)/3.97(FP) | 3.72(TAG)/3.79(FP) | β |
| NLC 10 | 4.66(TAG)/4.62(FP) | 4.20(TAG) | 3.81(TAG)/3.97(FP) | – | $\beta' + \beta$ |
| NLC 11 | 4.62(TAG)/4.62(FP) | – | 3.88(TAG)/3.97(FP) | 3.72(TAG)/3.79(FP) | β |
| NLC 12 | 4.66(TAG)/4.62(FP) | 4.20(TAG) | 3.81(TAG)/3.97(FP) | – | $\beta' + \beta$ |
| NLC 13 | 4.66(TAG)/4.62(FP) | 4.20(TAG) | 3.81(TAG)/3.97(FP) | – | $\beta' + \beta$ |
| NLC 14 ^{***} | – | – | – | – | – |

*Short spacings characteristic of the triacylglycerols.

**Short spacings characteristic of the free phytosterols.

***Sample does without solid lipids, with only HOSO and FP.

varying only in the composition of the solid lipids, it was observed that in NLC 1 and NLC 4 compounds only by CA, the β -form was maintained. In NLC 3 and NLC 6 composed only with CR, the polymorphic transitions were delayed from $\beta' + \beta$ to β' . In NLC 2 and NLC 5 composed by the mixture of CA and CR, the polymorphic transition was accelerated to the β -form. According to Oliveira, Stahl, Ribeiro, Grimaldi, Cardoso, and Kieckbusch (2015), the polymorphic behavior of CA is the β -form, and according to Ribeiro et al. (2013), the polymorphic behavior of CR is the mixture of crystals in forms β' and β . Thus, it can be affirmed that these results, even with the interference of the FP peaks, have agreed with the crystallization behavior of the lipid raw materials used in the formulation of LMs and NLCs. Notably, NLC 3 and NLC 6 will probably undergo polymorphic transition, presenting a mixture of $\beta' + \beta$ forms, according to the polymorphic behavior of CR.

Similar results regarding the composition of the hardfat were found for the NLCs containing 50% FP. NLC 10, NLC 12, and NLC 13, composed of CR, CA + CR, and CR, respectively, presented a mixture of crystals in the $\beta' + \beta$ forms, whereas NLC 8, NLC 9, and NLC 11, composed of CA, CA + CR, and CA, respectively, showed crystals in the most stable β -form. The use of CR enabled the development of NLC with the β -form and the mixture of polymorphic forms β' and β . Therefore, it can extend the applications in foods, e.g., in margarine or spreads, where form β' is desirable. According to Sato (2001), the crystals in form β' contribute to the formation of softer fats, with good aeration and properties of creaminess.

4. Conclusion

LMs developed with CA and CR and with HOSO presented promising prospects for the development of NLCs for the incorporation of bioactive compounds. For the development of NLCs with FP, the LMs composed of CA and CR separately in the formulations showed adequate thermal behaviors, where it was possible to verify the complete incorporation of FP. The incorporation of FP promoted the increase in the thermal resistance of LMs, increasing also the crystallinity of the developed systems. Notably, in this study, the incorporation of high levels of FP in the lipid nanoparticles was effective. The NLCs developed with 30% FP incorporation presented the best results regarding Z-ave, PDI, and ZP compared to those of the NLCs with 50% FP during 60 days of evaluation. The NLCs obtained with the polymorphic β' -form can be applied in food products, where soft and creamy properties are desired. In this study, was highlighted that the use of natural raw materials, such as vegetable oils and fats confer different characteristics depending on the vegetable source. In this way, is suggested for new experiments to extend the use of other vegetable oils and fats to obtain nanostructured systems with different crystalline characteristics and thermal stability for applications in different food products.

Declaration of Competing Interest

None.

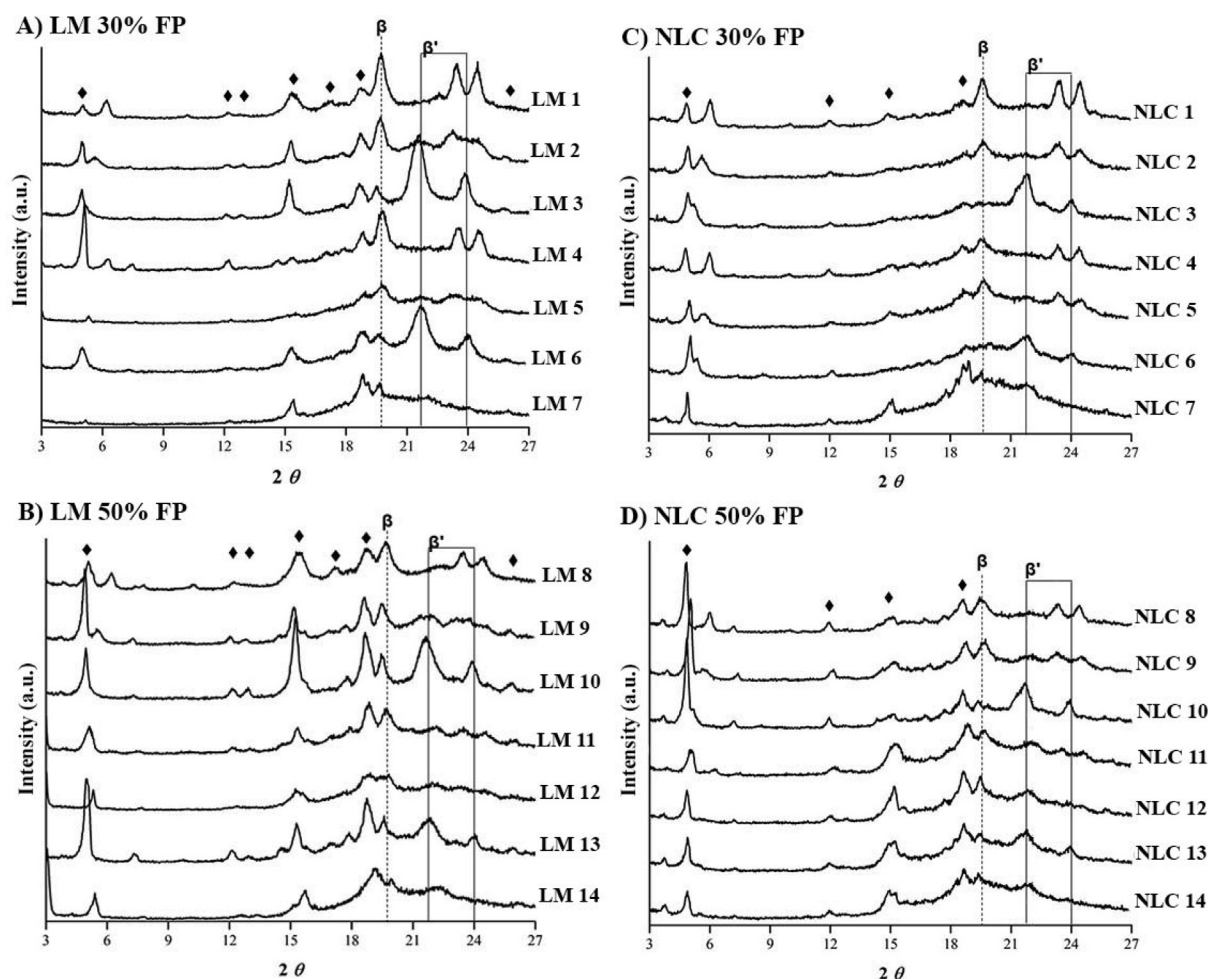


Fig. 4. X-ray diffraction patterns from: A) Lipid matrices (LMs) developed with the fully hydrogenated canola (CA) and/or crambe (CR) oils, and/or high oleic sunflower oil (HOSO) containing 30% of free phytosterols (FP); B) LMs developed with CA and/or CR, and/or HOSO containing 50% of FP; C) Nanostructured lipid carriers (NLCs) with 30% of FP; D) NLCs with 50% of FP.

Acknowledgements

The authors are grateful for the financial support of the Foundation for Research Support of the State of São Paulo (FAPESP, Brazil) referring to case 16/11261-8 and the doctoral scholarship of the Coordination for the Improvement of Higher Education Personnel (CAPES, Brazil).

Appendix A. Supplementary data

Supplementary data to this article can be found online at <https://doi.org/10.1016/j.foodchem.2019.125053>.

References

- Aditya, N. P., Aditya, S., Yang, H., Kim, H. W., Park, S. O., & Ko, S. (2015). Co-delivery of hydrophobic curcumin and hydrophilic catechin by a water-in-oil-in-water double emulsion. *Food Chemistry*, 173, 7–13.
- AOCS (2009). *Official methods and recommended practices of the American Oil Chemists' Society*. Urbana (USA): AOCS Press.
- Awad, T. S., Helgason, T., Weiss, J., Decker, E. A., & McClements, D. J. (2009). Effect of Omega-3 fatty acids on crystallization, polymorphic transformation and stability of tripalmitin solid lipid nanoparticle suspensions. *Crystal Growth & Design*, 9(8), 3405–3411.
- Beloqui, A., Solinis, M. A., Rodriguez-Gascon, A., Almeida, A. J., & Preat, V. (2016). Nanostructured lipid carriers: Promising drug delivery systems for future clinics. *Nanomedicine*, 12(1), 143–161.
- Bunjes, H., & Unruh, T. (2007). Characterization of lipid nanoparticles by differential scanning calorimetry, X-ray and neutron scattering. *Advanced Drug Delivery Reviews*, 59(6), 379–402.
- Cerqueira, M. A., Pinheiro, A. C., Silva, H. D., Ramos, P. E., Azevedo, M. A., Flores-López, M. L., ... Vicente, A. A. (2014). Design of bio-nanosystems for oral delivery of functional compounds. *Food Engineering Reviews*, 6(1–2), 1–19.
- Gomes Silva, M., Santos, V. S., Fernandes, G. D., Calligaris, G., Santana, M. H. A., Cardoso, L. P., & Ribeiro, A. P. B. (2019). Physical approach for a quantitative analysis of the phytosterols in free phytosterol-oil blends by X-ray Rietveld method. *Food Research International*. <https://doi.org/10.1016/j.foodres.2019.04.006>.
- Vaikousi, Hariklia, Lazaridou, Athina, Biliaderis, Costas G., & Zawistowski, J. (2007). Phase transitions, solubility, and crystallization kinetics of phytosterols and phytosterol-oil blends. *Journal of Agricultural and Food Chemistry*, 55, 1790–1798.
- Himawan, C., Starov, V. M., & Stapley, A. G. (2006). Thermodynamic and kinetic aspects of fat crystallization. *Advances in Colloid and Interface Science*, 122(1–3), 3–33.
- Kritchevsky, D., & Chen, S. C. (2005). Phytosterols—health benefits and potential concerns: A review. *Nutrition Research*, 25(5), 413–428.
- Lacatusu, I., Badea, N., Stan, R., & Meghea, A. (2012). Novel bio-active lipid nanocarriers for the stabilization and sustained release of sitosterol. *Nanotechnology*, 23(45), 455702.
- Lacatusu, I., Mitrea, E., Badea, N., Stan, R., Oprea, O., & Meghea, A. (2013). Lipid nanoparticles based on omega-3 fatty acids as effective carriers for lutein delivery. Preparation and in vitro characterization studies. *Journal of Functional Foods*, 5(3), 1260–1269.
- Li, J., Ho, C.-T., Li, H., Tao, H., & Tao, L. (2000). Separation of sterols and triterpene alcohols from unsaponifiable fractions of three plant seed oils. *Journal of Food Lipids*, 7(1), 11–20.
- Ling, W. H., & Jones, P. J. (1995). Dietary phytosterols: A review of metabolism, benefits and side effects. *Life Science*, 57(3), 195–206.
- Madureira, A. R., Campos, D., Gullon, B., Marques, C., Rodriguez-Alcala, L. M., Calhau, C., ... Pintado, M. (2016). Fermentation of bioactive solid lipid nanoparticles by human gut microflora. *Food & Function*, 7(1), 516–529.
- Martini, S., Awad, T., & Marangoni, A. G. (2006). Structure and properties of fat crystals networks. In F. Gunstone (Ed.), *Modifying lipids for use in foods* (pp. 142–169). NY: CRC Press.
- Moruisi, K. G., Oosthuizen, W., & Opperman, A. M. (2013). Phytosterols/stanols lower

- cholesterol concentrations in familial hypercholesterolemic subjects: A systematic review with meta-analysis. *Journal of the American College of Nutrition*, 25(1), 41–48.
- Ntanios, F. Y., MacDougall, D. E., & Jones, P. J. (1998). Gender effects of tall oil versus soybean phytosterols as cholesterol-lowering agents in hamsters. *Canadian Journal of Physiology and Pharmacology*, 76(7-8), 780–787.
- Oliveira, G. M.d., Stahl, M. A., Ribeiro, A. P. B., Grimaldi, R., Cardoso, L. P., & Kieckbusch, T. G. (2015). Development of zero trans/low sat fat systems structured with sorbitan monostearate and fully hydrogenated canola oil. *European Journal of Lipid Science and Technology*, 117(11), 1762–1771.
- Rashidi, L., & Khosravi-Darani, K. (2011). The applications of nanotechnology in food industry. *Critical Reviews in Food Science and Nutrition*, 51, 723–730.
- Ribeiro, A. P. B., Basso, R. C., & Kieckbusch, T. G. (2013). Effect of the addition of hardfats on the physical properties of cocoa butter. *European Journal of Lipid Science and Technology*, 115, 301–312.
- Rousseau, A. G., & Marangoni, A. (2002). *Food lipids: Chemistry, nutrition, and biotechnology*. New York: CRC Press.
- Salminen, H., Helgason, T., Kristinsson, B., Kristbergsson, K., & Weiss, J. (2013). Formation of solid shell nanoparticles with liquid omega-3 fatty acid core. *Food Chemistry*, 141(3), 2934–2943.
- Santos, V. S., Ribeiro, A. P. B., & Santana, M. H. (2019). Solid lipid nanoparticles as carriers for lipophilic compounds for applications in foods. *Food Research International*, 122, 610–626. <https://doi.org/10.1016/j.foodres.2019.01.032>.
- Santos, V. S., Ribeiro, A. P. B., & Santana, M. H. A. (2017). Nanopartículas Lipídicas Sólidas (NLS) e Carreadores Lipídicos Nanoestruturados (CLN) para aplicação em alimentos, processo para obtenção de NLS e CLN e uso das NLS e dos CLN. In Unicamp (Ed.), INPI - Instituto Nacional da Propriedade Industrial, vol. BR 10 2017 006471 9, Brasil, pp. 40.
- Sato, K. (2001). *Crystallization behaviour of fats and lipids: A review*. Oxford.
- Shahzad, N., Khan, W., Md, S., Ali, A., Saluja, S. S., Sharma, S., ... Al-Ghamdi, S. S. (2017). Phytosterols as a natural anticancer agent: Current status and future perspective. *Biomedicine & Pharmacotherapy*, 88, 786–794.
- Sharma, V. K., Diwan, A., Sardana, S., & Dhall, V. (2011). Solid lipid nanoparticles system: An overview. *International Journal of Research in Pharmaceutical Sciences*, 2(3), 450–461.
- Tamjidi, F., Shahedi, M., Varshosaz, J., & Nasirpour, A. (2013). Nanostructured lipid carriers (NLC): A potential delivery system for bioactive food molecules. *Innovative Food Science & Emerging Technologies*, 19, 29–43. <https://doi.org/10.1016/j.ifset.2013.03.002>.
- Villaseñor, I. M., Angelada, J., Canlas, A. P., & Echegoyen, D. (2002). Bioactivity studies on β -sitosterol and its glucoside. *Phytotherapy Research*, 16(5), 417–421.
- Wang, J. L., Dong, X. Y., Wei, F., Zhong, J., Liu, B., Yao, M. H., ... Chen, H. (2014). Preparation and characterization of novel lipid carriers containing microalgae oil for food applications. *Journal of Food Science*, 79(2), E169–E177.
- Weiss, J., Decker, E. A., McClements, D. J., Kristbergsson, K., Helgason, T., & Awad, T. (2008). Solid lipid nanoparticles as delivery systems for bioactive food components. *Food Biophysics*, 3(2), 146–154.
- Weiss, J., Takhistov, P., & McClements, D. J. (2006). Functional materials in food nanotechnology. *Journal of Food Science*, 71(9), R107–R116.
- Wu, T., Fu, J., Yang, Y., Zhang, L., & Han, J. (2009). The effects of phytosterols/stanols on blood lipid profiles: A systematic review with meta-analysis. *Asia Pacific Journal of Clinical Nutrition*, 18(2), 179–186.